

Two-dimensional Bose and Fermi gases beyond weak coupling

Guilherme França,¹ André LeClair,¹ and Joshua Squires¹

¹ *Department of Physics, Cornell University, Ithaca, NY*

Using a formalism based on the two-body S-matrix we study two-dimensional Bose and Fermi gases with both attractive and repulsive interactions. Approximate analytic expressions, valid at weak coupling and beyond, are developed and applied to the Berezinskii-Kosterlitz-Thouless (BKT) transition. We successfully recover the correct logarithmic functional form of the critical chemical potential and density for the Bose gas. For fermions, the BKT critical temperature is calculated in BCS and BEC regimes through consideration of Tan's contact.

PACS numbers: 05.45.Mt, 03.75.Mn, 03.67.-a

I. INTRODUCTION

The absence of conventional long range order in two-dimensional (2D) systems is well known to be a consequence of low energy fluctuations [1, 2]. Phase transitions at finite temperature in 2D are instead marked by a topological order as described by Berezinskii, Kosterlitz, and Thouless (BKT) [3, 4]. Quasi long range order is exhibited below the BKT transition temperature, where spatial correlations of the order parameter decay algebraically rather than exponentially. The destruction of this ordering, due to the unpairing of vortices, has been observed experimentally using atomic gases [5].

Ultracold atomic gases are well suited for the exploration of BKT theory, as they can be effectively constrained to 2D [6–13] using an optical lattice or harmonic trap, and because their interactions are highly tunable through the use of Feshbach resonances. Theoretical studies of BKT physics in two dimensions using quantum gases are numerous. Fermi gases have been used to explore Cooper pairing and superconductivity in 2D [14, 15], as well as the normal Fermi liquid phase [16–18]. The superfluid transition and critical point of the 2D Fermi gas have also been treated [19, 20, 23]. Bose Einstein condensation in 2D, particularly at weak coupling, has been widely studied [21, 22]. The critical point of the 2D Bose gas has

been obtained in this limit through classical ϕ^4 theory [24–26], and with a renormalization group (RG) approach [27]. An RG analysis has also been used to examine the ground state of the Bose gas in arbitrary dimension [28].

In this paper we apply the formalism developed in [29] to study two-dimensional Bose and Fermi gases with both attractive and repulsive interactions. Inspired by the Yang-Yang equations of the Thermodynamical Bethe Ansatz [30], the formalism is centered around an integral equation with a kernel based on the logarithm of the two-body S-matrix. The main advantage of our approach is that the two-dimensional integral equation admits approximate analytic solutions in terms of the Lambert W function. Furthermore these approximate solutions remain useful beyond weak coupling, and as detailed in section III, they can be used to calculate any thermodynamic quantity of interest. In this work we primarily use this correspondence to calculate the critical points of the BKT transition for both Bose and Fermi gases. Below we summarize our chosen models, couplings, and formalism before describing our main results in sections IV and V.

II. RENORMALIZATION GROUP, PHYSICAL COUPLINGS, AND THERMODYNAMIC SCALING FUNCTIONS

The models considered in this paper are the simplest models of non-relativistic bosons and fermions with quartic interactions. The bosonic model is defined by the following action for a complex scalar field ϕ :

$$S = \int d^2\mathbf{x} dt \left(i\phi^\dagger \partial_t \phi - \frac{|\vec{\nabla}\phi|^2}{2m} - \frac{g}{4}(\phi^\dagger \phi)^2 \right). \quad (1)$$

For fermions, due to the fermionic statistics, one needs at least a 2-component field $\psi_{\uparrow,\downarrow}$:

$$S = \int d^2\mathbf{x} dt \left(\sum_{\alpha=\uparrow,\downarrow} i\psi_\alpha^\dagger \partial_t \psi_\alpha - \frac{|\vec{\nabla}\psi_\alpha|^2}{2m} - \frac{g}{2}\psi_\uparrow^\dagger \psi_\uparrow \psi_\downarrow^\dagger \psi_\downarrow \right). \quad (2)$$

In both cases, positive (negative) g corresponds to repulsive (attractive) interactions.

Although classically the coupling g is dimensionless, in the quantum theory it is not exactly marginal, i.e. it has a renormalization group (RG) flow. One way to determine the beta function is to calculate the exact 2-body S-matrix [29]. Multi-loop Feynman diagrams are divergent, and can be regularized with an ultraviolet cutoff Λ in momentum space \mathbf{k} .

The result is

$$\frac{dg}{d \log \Lambda} = \frac{mg^2}{4\pi}. \quad (3)$$

The above beta function is exact, i.e. there are no higher order corrections. It is characteristic of Berezinskii-Kosterlitz-Thouless transitions. For g positive, it is marginally irrelevant in that at low energies g flows to zero, whereas g negative is marginally relevant, i.e. g flows to $-\infty$.

There is a characteristic momentum scale in the problem, which plays the role of the physical coupling,

$$\Lambda_* = \Lambda e^{4\pi/mg}. \quad (4)$$

Since it is an RG invariant

$$\frac{d\Lambda_*}{d \log \Lambda} = 0. \quad (5)$$

The two-body S-matrix can be expressed entirely in terms of this scale:

$$S(|\mathbf{k}|) = \frac{4\pi/mg + \log(2\Lambda/|\mathbf{k}|) - i\pi/2}{4\pi/mg + \log(2\Lambda/|\mathbf{k}|) + i\pi/2} \quad (6)$$

$$= \frac{\log(2\Lambda_*/|\mathbf{k}|) - i\pi/2}{\log(2\Lambda_*/|\mathbf{k}|) + i\pi/2}, \quad (7)$$

where $|\mathbf{k}| = |\mathbf{k}_1 - \mathbf{k}_2|$ is the relative momentum of the two incoming particles. Note that because the two-body S-matrix can be calculated to all orders in the coupling, the second virial coefficient can be obtained exactly within our formalism, as explained in the appendix.

We will define the physical scattering length a_s as

$$a_s = \frac{1}{\Lambda_*} = \frac{1}{\Lambda} e^{-4\pi/mg}. \quad (8)$$

In two dimensions, this choice is really just a convention. Comparing the scattering amplitude based on the above S-matrix and the calculation in [27], the convention in the latter is $a_s = e^{-\gamma_E}/\Lambda_*$, where γ_E is the Euler-Mascheroni constant.

Thus as $g \rightarrow 0^+$, i.e. approaches zero from above, the scattering length $a_s \rightarrow 0$. On the other hand $a_s \rightarrow \infty$ as $g \rightarrow 0^-$. Strong coupling, $g \rightarrow \pm\infty$ just corresponds to a finite $a_s = 1/\Lambda$. Note that a negative scattering length is not physically possible, unlike in three dimensions. For reference, the parameters in the weak and strong coupling limits are summarized in Table I.

It is not physically meaningful to express properties in terms of g since it is not a renormalization group invariant; rather they should be expressed in terms of the scattering length

TABLE I: The parameter α is defined below in (9). The weak coupling limit is obtained with $\alpha \rightarrow \infty$ for repulsive interactions and $\alpha \rightarrow 0$ for attractive interactions. The strong coupling limit corresponds to finite α in both cases. \tilde{g} , defined in (13), is also finite at strong coupling.

	weak coupling			strong coupling		
	g	a_s	α	g	a_s	α
repulsive	0^+	0	∞	$+\infty$	$1/\Lambda^*$	$\mathcal{O}(1)$
attractive	0^-	∞	0^+	$-\infty$	$1/\Lambda^*$	$\mathcal{O}(1)$

a_s . At finite temperature and density, it is convenient to define the dimensionless variables:

$$\alpha = \frac{\lambda_T}{a_s}, \quad \tilde{\mu} = \frac{\mu}{T} \quad (9)$$

where $\lambda_T = \sqrt{2\pi/mT}$ is the thermal de Broglie wavelength and μ the chemical potential. The scaled density

$$\tilde{n} = n\lambda_T^2 \quad (10)$$

is a function of $\tilde{\mu}$ and α . For the full equation of state involving pressure, one also needs the free energy density:

$$\mathcal{F} = -\frac{\pi^2}{6} T \lambda_T^{-2} c(\tilde{\mu}, \alpha) \quad (11)$$

where c is defined below. With the above normalization, $c = 1$ for a free boson at zero chemical potential. In two dimensions the Fermi wave-vector is $k_F = \sqrt{2\pi n} = \lambda_T^{-1} \sqrt{2\pi \tilde{n}}$ and the Fermi temperature $T_F = \pi n/m$, which implies $T/T_F = 2/\tilde{n}$. In units of the Fermi energy, the energy per particle takes the form

$$\frac{E}{N} = \frac{\pi^2}{12} \left(\frac{T}{T_F} \right)^2 c(\tilde{\mu}, \alpha). \quad (12)$$

For comparison with other calculations and experiments, it is also useful to define a physical coupling \tilde{g} as

$$\tilde{g} = \frac{8\pi}{|\log(na_s^2)|} = \frac{8\pi}{|\log(\tilde{n}/\alpha^2)|} = \frac{4\pi}{\left| \log \left(\frac{k_F a_s}{\sqrt{2\pi}} \right) \right|} \quad (13)$$

The above definition is such that at weak coupling $\tilde{g} \approx g$.

III. FORMALISM

In the formalism developed in [29], thermodynamic functions are determined by a pseudo-energy $\varepsilon(\mathbf{k})$ which represents a single particle energy in the presence of interactions with all the other particles in the gas. The occupation numbers take the free particle form

$$f(\mathbf{k}) = \frac{1}{e^{\beta\varepsilon(\mathbf{k})} - s}, \quad n = \int \frac{d^2\mathbf{k}}{(2\pi)^2} f(\mathbf{k}) \quad (14)$$

where $s = 1$ ($s = -1$) corresponds to bosons (fermions). Consistent re-summation of all two particle interactions leads to an integral equation for $\varepsilon(\mathbf{k})$. It is convenient to define the function

$$y(\mathbf{k}) = e^{-(\varepsilon(\mathbf{k}) - \omega_{\mathbf{k}} + \mu)/T} \quad (15)$$

where $\omega_{\mathbf{k}} = \mathbf{k}^2/2m$. Without interactions, $y = 1$. With interactions y satisfies the non-linear integral equation

$$y(\mathbf{k}) = 1 + \frac{1}{T} \int \frac{d^2\mathbf{k}'}{(2\pi)^2} G_{\pm}(\mathbf{k} - \mathbf{k}') \frac{z}{e^{\omega_{\mathbf{k}'}/T} - szy(\mathbf{k}')} \quad (16)$$

where $z = e^{\mu/T}$, and G_{\pm} refers to bosons or fermions, respectively, with $G_- = G_+/2$. Henceforth G without a subscript will refer to G_+ . The fermionic case will be studied in section V.

The kernel G is related to the logarithm of the two-body S-matrix,

$$\begin{aligned} G(\mathbf{k} - \mathbf{k}') &= -\frac{4i}{m} \log S(\mathbf{k} - \mathbf{k}') \\ &= \frac{8}{m} \operatorname{arccot} \left[\frac{2}{\pi} \log(a_s |\mathbf{k} - \mathbf{k}'|/2) \right]. \end{aligned} \quad (17)$$

Rescaling $\mathbf{k} \rightarrow \sqrt{2mT} \mathbf{k}$, the scaling functions are then given by the following integrals ($k = |\mathbf{k}|$):

$$\tilde{n} = 2 \int_0^{\infty} dk k \frac{y(k)z}{e^{k^2} - sy(k)z}, \quad (18)$$

$$c = -\frac{12}{\pi^2} \int_0^{\infty} dk k \left[s \log \left(1 - szy(k)e^{-k^2} \right) + \frac{1}{2} \frac{z(y(k) - 1)}{e^{k^2} - szy(k)} \right]. \quad (19)$$

The integral equation (16) then becomes

$$y(k) = 1 + \frac{m}{2\pi^2} \int d^2\mathbf{k}' G(\mathbf{k} - \mathbf{k}') \frac{z}{e^{k'^2} - szy(k')}, \quad (20)$$

where the kernel is

$$G(\mathbf{k} - \mathbf{k}') = \frac{8}{m} \operatorname{arccot} \left[\frac{2}{\pi} \log \left(\frac{\sqrt{\pi} |\mathbf{k} - \mathbf{k}'|}{\alpha} \right) \right]. \quad (21)$$

The free theory limit corresponds to *both*, $\alpha \rightarrow \infty$ ($g \rightarrow 0^+$) and $\alpha \rightarrow 0$ ($g \rightarrow 0^-$). It will be convenient to write the integral equation (20) as

$$y(k) = 1 + \int_0^\infty dk' k' H(k, k') \frac{z}{e^{k'^2} - sz y(k')}, \quad (22)$$

where

$$H(k, k') = \frac{4}{\pi^2} \int_0^{2\pi} d\theta \operatorname{arccot} \left[\frac{1}{\pi} \log \left(\frac{\pi(k^2 + k'^2 - 2kk' \cos \theta)}{\alpha^2} \right) \right]. \quad (23)$$

In theory the integral equation (16) is valid for all interaction strengths and temperatures, including $T = 0$. However, as our formalism only includes a pseudo-energy for single particles, the integral equation is only solvable in the absence of bound states, limiting its applicability at zero temperature. Low temperature results are accurate only if the gas remains in the normal phase. As a concrete example, we calculated Tan's contact for the attractive Fermi gas in the normal phase for temperatures as low as $T/T_F = 0.001$ (see Figure 5 and the discussion in Section V).

We also expect solutions of the integral equation to become less reliable if the coupling is large enough to result in appreciable many-body interactions, as only two-body effects are considered. If we take as a measure of strong versus weak coupling the constant \tilde{g} defined in (13), then because of the logarithm, $\tilde{g} \approx 1$ requires (for repulsive interactions) a very large α , on the order of 10^6 (see below). For such large α , in practice we can disregard the momentum dependence of the above kernel. We checked numerically that retaining the k dependence did not substantially alter our results below. Thus, henceforth

$$H \approx \frac{8}{\pi} \operatorname{arccot} \left[-\frac{2}{\pi} \log \alpha \right] \approx -\frac{4}{\log \alpha} \rightarrow 0^\pm. \quad (24)$$

is a constant that differs in sign depending on whether the interaction is attractive or repulsive.

IV. BOSONS

Since the kernel is a constant, y is also a constant. The integral over k can be performed and the integral equation (22) becomes the transcendental equation

$$y(y - 1) = \frac{2 \log(1 - yz)}{\log \alpha}. \quad (25)$$

The equation of state is then

$$\tilde{n} = -\log(1 - yz). \quad (26)$$

Given the solution to (25) for y as a function of z , the above equation determines how the density depends on the chemical potential and temperature.

For very weak coupling, $y \approx 1$, and (25) can be approximated as

$$y = 1 + \frac{2 \log(1 - yz)}{\log \alpha} \quad (27)$$

which can be expressed in terms of the Lambert W -function. The W function by definition satisfies

$$W(u)e^{W(u)} = u. \quad (28)$$

One then has the following solution of the transcendental equation:

$$y = 1 - a \log(1 - y/b) \quad \Rightarrow \quad y = b + aW \left(-\frac{b}{a} e^{(1-b)/a} \right). \quad (29)$$

Thus

$$y = \frac{1}{z} - \frac{2}{\log \alpha} W \left(\frac{\log \alpha}{2z} e^{(1/z-1) \log \sqrt{\alpha}} \right). \quad (30)$$

For real u , $W(u)$ has two real valued branches, as shown in Figure 1 below. If $u \geq 0$ there is only the principal branch denoted by $W_0(u)$, and if $-1/e \leq u < 0$ we have the principal branch W_0 and also the secondary branch $W_{-1}(u)$. The two branches only coincide when $u = -1/e$, where $W_0(-1/e) = W_{-1}(-1/e) = -1$.

A. Repulsive Bosons

For the repulsive case the argument of W is positive and one should chose the principle branch, henceforth simply denoted as W .

In order to compare with other theories and experiments, we wish to plot \tilde{n} as a function of $\tilde{\mu}$ for various \tilde{g} . The above equations give explicit expressions in terms of α rather

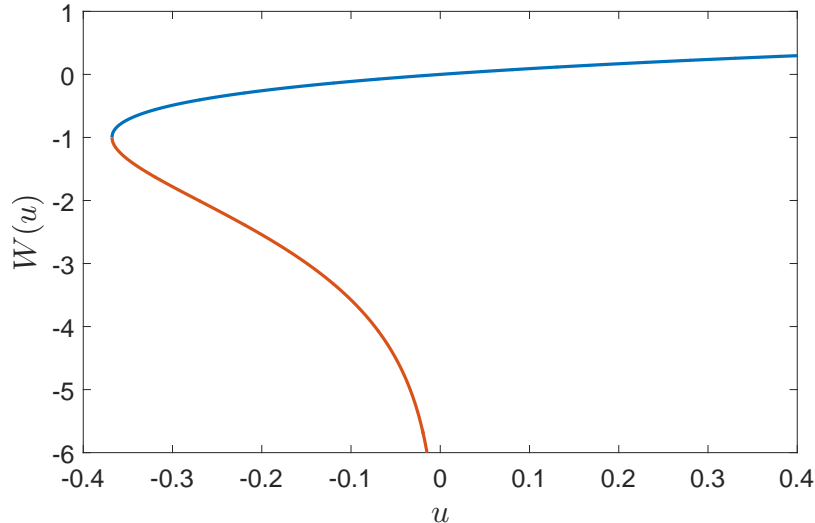


FIG. 1: (color online) The two real branches of the Lambert W -function. The top blue part is the principal branch $W_0(u)$, whereas the lower orange part is $W_{-1}(u)$. The branches meet at $u = -1/e$.

than \tilde{g} . However the primary variation of \tilde{g} comes from the variation of α . Therefore we plot \tilde{n} as a function $\tilde{\mu}$ for a fixed α . Along such a curve \tilde{g} is nearly constant, thus it is meaningful to associate each fixed- α curve with $\tilde{g}_0 = \tilde{g}(\tilde{\mu} = 0^-, \alpha)$. Our results, which use the approximation (30), are compared to experimental data in Figure 2 for \tilde{g}_0 ranging between 0.05 and 0.66. Due to the logarithms, this requires a very large range of α . For instance $\tilde{g}_0 = 0.05$ corresponds to $\alpha \approx 10^{110}$ whereas $\tilde{g}_0 = 0.66$ coincides with $\alpha \approx 10^8$.

As $\tilde{\mu} \rightarrow -\infty$ the behavior is of a free gas $\tilde{n} \approx -\log(1 - z)$. There are significant downshifts at finite $\tilde{\mu}$ which increase with \tilde{g} . These results compare reasonably well with the measurements in [13].

At some critical density \tilde{n}_c the gas is known to become a superfluid. In order to motivate our analysis of the critical point, let us consider ordinary BEC of free particles in three spatial dimensions. Here the kernel $G = 0$, and $y(\mathbf{k}) = 1$, which implies $\varepsilon(\mathbf{k}) = \omega(\mathbf{k}) - \mu$. At the critical point the occupation number $f(\mathbf{k} = 0)$ diverges, implying $\varepsilon(0) = \mu_c = 0$. This property is reflected in the analytic properties of the density as a function of z as follows. One has $\tilde{n} = n\lambda_T^3 = \text{Li}_{3/2}(z)$ where Li is the polylogarithm. The latter has a branch cut along the real axis $\text{Re}(z) > 1$ where the density \tilde{n} develops an imaginary part. Therefore the critical point is $z_c = 1$ and $\tilde{n}_c = \text{Li}_{3/2}(z_c) = \zeta(3/2)$ where ζ is the Riemann zeta function. In two dimensions this leads to $\zeta(1)$ which diverges due to the pole of ζ at $z = 1$.

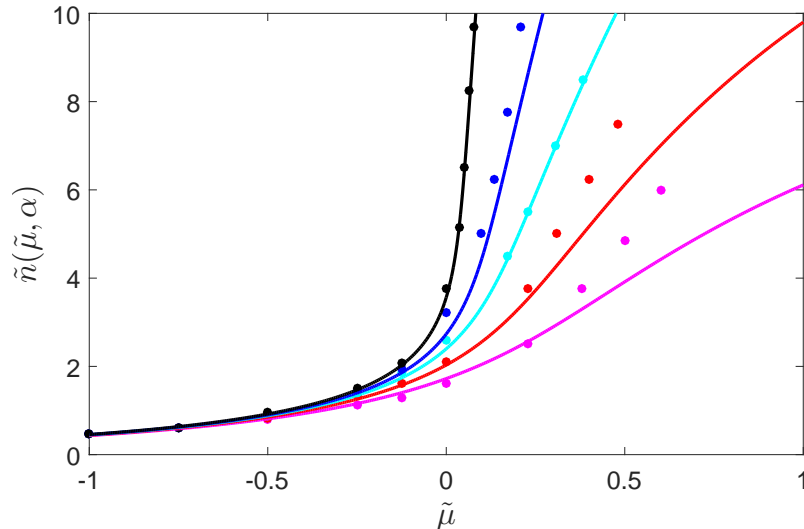


FIG. 2: (color online) The scaled density \tilde{n} as a function of the scaled chemical potential $\tilde{\mu}$ for various \tilde{g}_0 . From top to bottom, the solid colored lines correspond to $\tilde{g}_0 = 0.05, 0.15, 0.24, 0.41, 0.66$ respectively. The colored points, which have the same ordering from top to bottom, are experimental data estimated from [13].

For a two dimensional interacting gas, as in the 3D non-interacting case, at the critical point the scaled density \tilde{n} develops an imaginary part. This occurs for $y \approx 1/z$ where the RHS of (25) has a branch cut. In order to study this analytically using known functions, we consider the approximate solution of (25) given by (30). Taking $y = 1/z_c$ implies

$$W\left(\frac{\log \sqrt{\alpha}}{z_c} e^{(1/z_c - 1) \log \sqrt{\alpha}}\right) = 0. \quad (31)$$

Since the argument of W is arbitrarily large and positive for weakly coupled repulsive interactions, the approximation $W_0(u) \approx \log u$ can be used, giving

$$\log\left(\frac{\log \sqrt{\alpha}}{z_c}\right) + \log \sqrt{\alpha} \left(\frac{1}{z_c} - 1\right) = 0. \quad (32)$$

The solution z_c to the above equation can again be expressed in terms of the Lambert W function

$$z_c = \frac{\log \sqrt{\alpha}}{W(\sqrt{\alpha})}. \quad (33)$$

Noting to second order, for large u , $W_0(u) \approx \log u - \log \log u$, one can use the above equation and (26) to compute the critical chemical potential and density:

$$\begin{aligned} \tilde{\mu}_c &\approx \frac{\log \log \sqrt{\alpha}}{\log \sqrt{\alpha}} \\ \tilde{n}_c &\approx \log \log \sqrt{\alpha}. \end{aligned} \quad (34)$$

We now compare (34) with known results and experiments. From the scattering length definition given by (8) we see $\log \sqrt{\alpha} \approx 2\pi/mg$. This leads to

$$\begin{aligned}\tilde{\mu}_c &\approx \frac{mg}{2\pi} \log \left(\frac{2\xi_\mu}{mg} \right) \\ \tilde{n}_c &\approx \log \left(\frac{2\xi}{mg} \right)\end{aligned}\tag{35}$$

with $\xi = \xi_\mu = \pi$. The above functional dependence on g agrees with [13, 25] except for the constants inside the logarithm, where it was found that $\xi_\mu \approx 13.2$ and $\xi \approx 380$. We do not understand the reason for this discrepancy. The simplest explanation is that we are neglecting intrinsic 3-body interactions and higher; however it is hard to see how these would lead to the same functional form as in (35) with just modifications of the ξ 's. It seems more likely to be an effect of our simplifications of the kernel in the integral equation, which effectively neglected its momentum dependence in the limit of large α . Although we did not find any significant evidence of this numerically, it remains possible that we did not treat the integral equation properly in the infra-red, i.e. low k .

B. Attractive Bosons

For attractive interactions in the weak coupling limit, (24) is positive, and $\alpha \rightarrow 0^+$. In this regime there exists only very small regions of parameter space where there is a solution to (25). This instability is reflected in the equation of state, as shown in Figure 3.

At the critical point, \tilde{n} again becomes complex. The main difference in repeating the analysis of the previous section is now, for attractive interactions, the argument of W in (30) is arbitrarily small and negative and one must choose the secondary branch rather than the principle branch. After setting $y = 1/z_c$ we find

$$W_{-1} \left(\frac{\log \sqrt{\alpha}}{z_c} e^{(1/z_c - 1) \log \sqrt{\alpha}} \right) = 0.\tag{36}$$

Utilizing the asymptotic expansion of the secondary branch $W_{-1}(-\frac{1}{u}) \approx -\log u - \log \log u$ gives

$$\log \left(\frac{|\log \sqrt{\alpha}|}{z_c} \right) - \left(\frac{1}{z_c} - 1 \right) |\log \sqrt{\alpha}| = 0,\tag{37}$$

from which it follows

$$z_c = \frac{\log \sqrt{\alpha}}{W_{-1}(-\sqrt{\alpha})}.\tag{38}$$

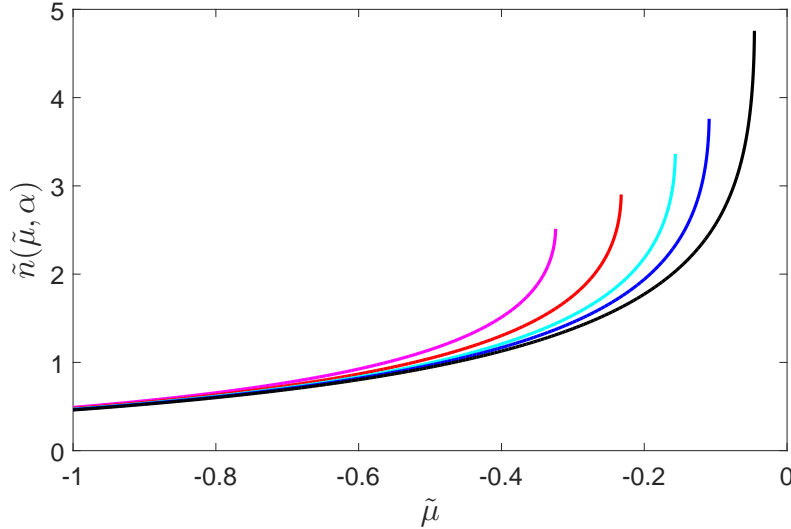


FIG. 3: (color online) The scaled density \tilde{n} as a function of the scaled chemical potential $\tilde{\mu}$ for various \tilde{g}_0 . From bottom to top, the solid colored lines correspond to $\tilde{g}_0 = 0.05, 0.15, 0.24, 0.41,$ and 0.66 respectively. Each \tilde{n} curve terminates at a specific chemical potential, after which no solution to (27) exists for larger values of $\tilde{\mu}$.

As in the repulsive case the critical density can be computed by inserting the above expression into (26). Using the asymptotic expansion of W_{-1} a second time results in

$$\begin{aligned}\tilde{\mu}_c &\approx \frac{-\log|\log\sqrt{\alpha}|}{|\log\sqrt{\alpha}|} \\ \tilde{n}_c &\approx \log|\log\sqrt{\alpha}|.\end{aligned}\tag{39}$$

V. FERMIONS

In the fermionic case the kernel $G_- = G_+/2$. The analogs of (25) and (26) for fermions at weak coupling are then

$$y(y-1) = -\frac{\log(1+yz)}{\log\alpha}\tag{40}$$

and

$$\tilde{n} = \log(1+yz).\tag{41}$$

Mirroring our treatment of bosons, we find approximate solutions for y in the attractive ($\alpha \rightarrow 0$)

$$y = -\frac{1}{z} + \frac{1}{\log\alpha} W_{-1}\left(\frac{\log\alpha}{z} e^{(1/z-1)\log\sqrt{\alpha}}\right)\tag{42}$$

and repulsive ($\alpha \rightarrow \infty$)

$$y = -\frac{1}{z} + \frac{1}{\log \alpha} W_0 \left(\frac{\log \alpha}{z} e^{(1/z-1) \log \sqrt{\alpha}} \right) \quad (43)$$

regimes in terms of the Lambert function.

A. Attractive Fermions

A useful quantity to calculate is the contact parameter, C , which is set by the antiparallel spin pair correlation function $g_{\uparrow\downarrow}(r)$ at short distances ($r \ll 1/k_F$). Tan's relations provide a connection between C , and thus the short range interactions of the system, and macroscopic quantities such as the pressure of the gas [31]. One can define a dimensionless contact in terms of a derivative of the energy with respect to the interaction parameter

$$C' = C/k_F^2 = \pi \frac{d \frac{E}{E_F}}{d \log(k_F a_s)}. \quad (44)$$

Note since $T/T_F = 2/\tilde{n}$ this derivative can be calculated explicitly with our formalism. Using the approximations given by (41) and (42):

$$C' = \frac{2\pi [\log \alpha^{(1+1/z)} - W_{-1}(v)]}{\log \left(\frac{zW_{-1}(v)}{\log \alpha} \right)^2 [\log \alpha (W_{-1}(v) + 1)]} \quad (45)$$

where $v = \alpha^{(1+1/z)} \log \alpha^{1/z}$.

For the 2D attractive fermi gas, the contact was recently measured experimentally at $T/T_F = 0.27$ [8]. In Figure 4 below we compare C' as calculated with our approximations to experiment, as well as to a $T = 0$ Fermi liquid theory result [17]. Our C' compares favorably with the experimental measurements until diverging abruptly as $\alpha \rightarrow 1$.

Since C' is proportional to the number of atomic pairs, which follows from the relation between the contact and $g_{\uparrow\downarrow}(r)$ [32], a divergence in C' may signal a phase transition. Identifying the critical point of the BKT transition with a diverging C' yields the phase diagram shown in Figure 5.

In the 2D BCS limit $\log(k_F a_s) \gg 1$, the critical temperature of the superfluid transition has been calculated using mean field theory [20, 23]

$$\frac{T_c}{T_F} = \frac{2e^{\gamma-1}}{\pi k_F a_s} = \frac{c_{MF}}{k_F a_s}. \quad (46)$$

Fitting our phase boundary to a second order model

$$\frac{T_c}{T_F} = \frac{c_1}{k_F a_s} + \frac{c_2}{(k_F a_s)^2} \quad (47)$$

gives $c_1 = 0.865 = 2.08c_{MF}$ and $c_2 = 6.07$. Our results begin to significantly depart from those of mean field theory around $\log(k_F a_s) = 3$ which corresponds to $\tilde{g} \approx 6$. This is well into the regime of strong interactions, so it's unsurprising we deviate from a mean field theory prediction.

Before considering repulsive interactions, we note that Monte Carlo simulations have been used to calculate both the contact and energy per particle at $T = 0$ on both sides of the BEC-BCS crossover. For example, in [33] for $\log(k_F a_s) = 5.18$, the normalized energy per particle is reported as $E/N = 0.821$. To compare to this data we calculate E/N using (12) at low temperature. For convenience we take $T/T_F = 0.01$, which fixes the density \tilde{n} . Since the interaction parameter $\log(k_F a_s)$ only depends on $\tilde{n}(\tilde{\mu}, \alpha)$ and α , setting $\log(k_F a_s) = 5.18$ uniquely determines α . With α and $\tilde{n}(\tilde{\mu}, \alpha)$ known, a corresponding $\tilde{\mu}$ can be found numerically, and used to calculate the energy per particle. Utilizing the approximations (41) and (42) throughout, we obtain $E/N = 0.995$. Although E/N is provided for a range of interaction strengths, most of the data presented in [33] occurs in the presence of a bound state, which our formalism is not suited to handle.

B. Repulsive Fermions

While we don't have experimental data to compare to on the BEC side, the contact is equivalent to (45) with $W(v)$ in place of $W_{-1}(v)$. As in the attractive case, a sharp increase in C' is observed (see Figure 6) which we take as indication of a phase transition. In the BEC limit of $\log(k_F a_s) \ll -1$, the predicted critical temperature is

$$\frac{T_c}{T_F} = \frac{1}{2} \left(\log \left(\frac{\xi}{2\pi} \log \left(\frac{2\sqrt{\pi}}{k_F a_s} \right) \right) \right)^{-1} \quad (48)$$

with $\xi = 380$ [23, 25]. We instead find T_c/T_F to be more consistent with the value $\xi = \pi$ from (35), as shown in Figure 7. The return of this discrepancy is expected based on the analysis in section IV, as in this limit the system behaves as a weak Bose gas.

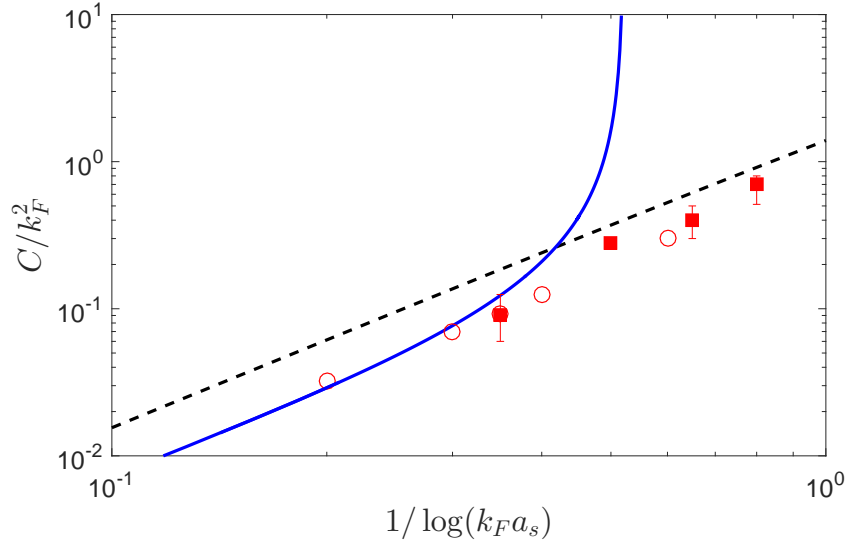


FIG. 4: Dimensionless contact C' vs. $1/\log(k_F a_s)$ at $T/T_F = 0.27$. The red squares and error bars are experimental data estimated from [8]. The red open circles are from the same group, but calculated from a model which accounts for their specific experimental configuration. The dashed black line is a 2nd order $T = 0$ homogenous Fermi liquid theory result, and the solid blue curve uses the Lambert approximation (42) to calculate C' .

VI. CONCLUSIONS

The S-matrix-based formalism developed in [29] has been applied to two-dimensional Bose and Fermi gases. The main obstacle in utilizing this method to extract measurable thermodynamic functions is solving an integral equation whose kernel takes a particularly complicated form in two dimensions. This makes exact solution of the integral equation an impossible task, and numerical treatments computationally intensive. Fortunately, in the limits $\alpha \ll 1$ and $\alpha \gg 1$ the momentum dependence of the kernel becomes irrelevant, and elegant solutions of the integral equation can be written in terms of the Lambert W function.

While we initially anticipated these approximate solutions would only remain valid in the limit of extremely weak coupling, it turns out \tilde{g} is a more appropriate measure of coupling strength than α , due to its explicit density dependence. For strong coupling, $\tilde{g} \gtrsim 1$ which is reached in the $\alpha \ll 1$ or $\alpha \gg 1$ limit depending on the sign of the interaction.

For bosons, we were able to recover the well-established logarithmic functional form of the critical density and chemical potential with the Lambert approximation, up to a constant

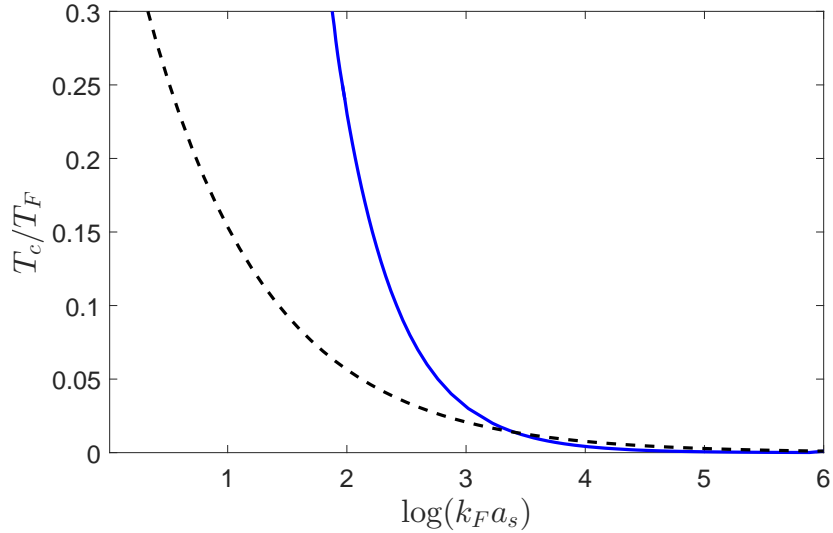


FIG. 5: T_c/T_F as a function of the interaction parameter $\log(k_F a_s)$. The dashed black line is the mean field theory result (46) and the blue is obtained through the method described in the text. Up to $\log(k_F a_s) \approx 3$ our T_c/T_F closely matches the mean field theory prediction.

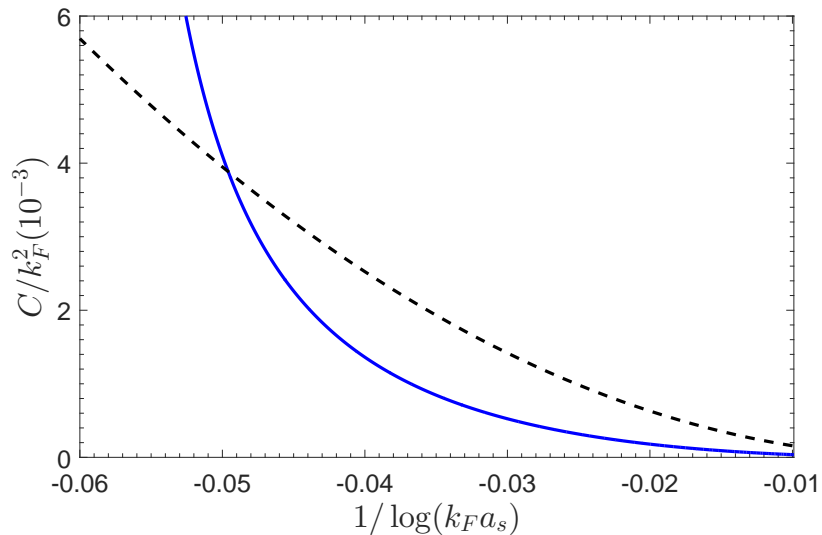


FIG. 6: Dimensionless contact C' vs. $1/\log(k_F a_s)$ at $T/T_F = 0.1$. The dashed black line is the 2nd order $T = 0$ homogenous Fermi liquid theory prediction, and the blue uses the Lambert approximation (43) to calculate C' .

obtained with Monte Carlo methods [25]. For fermions our approximations result in an explicit expression for the contact parameter, from which the critical temperature of the BKT transition has been deduced. This novel approach agrees with known weak coupling

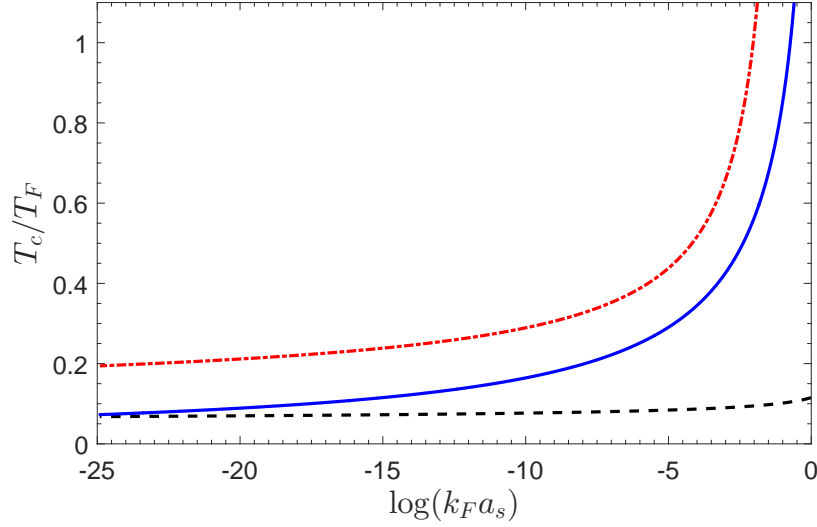


FIG. 7: T_c/T_F as a function of the interaction parameter $\log(k_F a_s)$. The dashed black line is the mean field theory result given by (48). The red dash-dot line uses the same model except with our previously calculated $\xi = \pi$ instead of $\xi = 380$. The solid blue curve is determined by the behavior of C' , as described in the text.

mean field theory calculations [20, 23].

As two-dimensional gases are poised to garner even greater attention in the near future, we hope our explicit analytic results are found to be useful.

ACKNOWLEDGMENTS

We thank John Stout for collaboration in the early stages of this work which led to the Appendix.

APPENDIX: VIRIAL EXPANSION

We did not use the following results in the body of the article, however we present them here since they may be useful in future studies.

The virial expansion is formally defined as a series expansion of \mathcal{F} in powers of the

fugacity z :

$$\begin{aligned} -\mathcal{F}\lambda_T^2/T &= \sum_{n=1}^{\infty} b_n z^n \\ n\lambda_T^2 &= \sum_{n=1}^{\infty} n b_n z^n \end{aligned} \quad (49)$$

where the second relation follows from $n = -\partial\mathcal{F}/\partial\mu$. In the free theory, the series expansion of the poly-logarithm $s\text{Li}_2(sz)$ gives $b_n = s^{n+1}/n^2$.

As explained in [34] our formalism gives the corrections to b_2 and b_3 :

$$\begin{aligned} b_2 &= \frac{s}{4} + \frac{\lambda_T^2}{2T} \int \frac{d^2\mathbf{k}}{(2\pi)^2} \frac{d^2\mathbf{k}'}{(2\pi)^2} \\ &\quad \times (e^{-\omega_{\mathbf{k}}/T} e^{-\omega_{\mathbf{k}'}/T} G_{\pm}(\mathbf{k} - \mathbf{k}')), \end{aligned} \quad (50)$$

$$\begin{aligned} b_3 &= \frac{1}{9} + \frac{s\lambda_T^2}{2T} \int \frac{d^2\mathbf{k}}{(2\pi)^2} \frac{d^2\mathbf{k}'}{(2\pi)^2} e^{-\omega_{\mathbf{k}}/T} e^{-\omega_{\mathbf{k}'}/T} G_{\pm}(\mathbf{k} - \mathbf{k}') \\ &\quad \times (e^{-\omega_{\mathbf{k}}/T} + e^{-\omega_{\mathbf{k}'}/T}). \end{aligned}$$

The second virial coefficient b_2 is exact, whereas b_3 is not since it does not contain the intrinsic 3-body physics. Hence we only consider b_2 . Rescaling $\mathbf{k} \rightarrow \sqrt{2mT}\mathbf{k}$, and making the change of variables $\mathbf{k}_1 = \mathbf{k} - \mathbf{k}'$, $\mathbf{k}_2 = \mathbf{k} + \mathbf{k}'$, the integral factorizes and the integral over \mathbf{k}_2 is simply a gaussian. The result is

$$b_2 = \frac{s}{4} + \frac{2\sigma}{\pi} \int_0^{\infty} dk k e^{-\frac{k^2}{2}} \text{arccot} \left[\frac{2}{\pi} \log \left(\frac{\sqrt{\pi} k}{\alpha} \right) \right] \quad (51)$$

where $k = |\mathbf{k}|$ and $\sigma = 1$ for bosons and $1/2$ for fermions. To a good approximation,

$$\begin{aligned} b_2(\alpha) &\approx \frac{s}{4} + \sigma \left(-1 + 2e^{-\alpha^2/2\pi} + \dots \right. \\ &\quad \left. \dots - \frac{2}{\pi} \arctan \left[\frac{1}{\pi} \log \left(\frac{2\pi \log 2}{\alpha^2} \right) \right] \right). \end{aligned} \quad (52)$$

Plots of b_2 are shown in Figure 8. Note that it changes sign at $\alpha \approx 2.65$. As expected, the free theory value $b_2 = s/4$ is approached in both limits $\alpha \rightarrow 0$ and $\alpha \rightarrow \infty$.

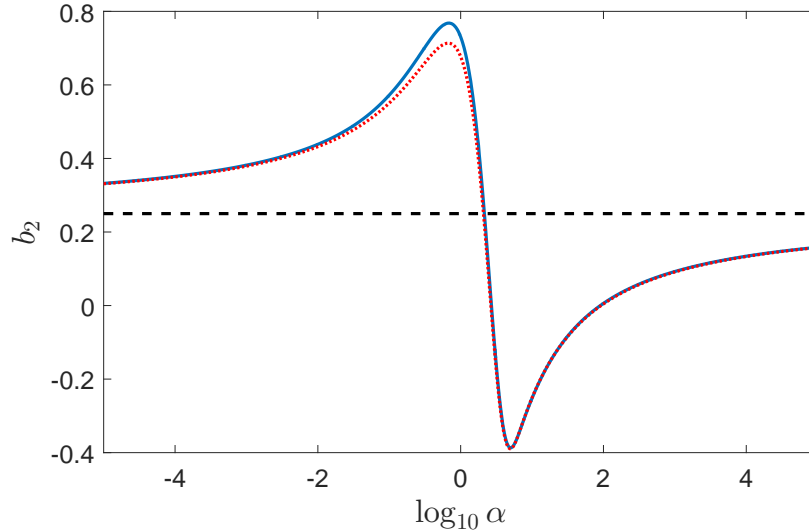


FIG. 8: The second virial coefficient b_2 as a function of α for bosons (solid blue). The dotted red curve is the approximation (52). The non-interacting value $b_2 = 1/4$ (dashed horizontal line) is approached as $\alpha \rightarrow 0$ and $\alpha \rightarrow \infty$.

-
- [1] N. D. Mermin and H. Wagner, *Absence of ferromagnetism or antiferromagnetism in one- or two-dimensional isotropic heisenberg models*, Phys. Rev. Lett. **17**, 1133-1136 (1966).
 - [2] P. C. Hohenberg, *Existence of long-range order in one and two dimensions*, Phys. Rev. **158**, 383-386 (1967)
 - [3] V. Berezinskii, Sov. Phys. JETP **34** 610 (1972).
 - [4] J. Kosterlitz and D. Thouless, J. Phys. C **6** 1181 (1973).
 - [5] Z. Hadzibabic, P. Krüger, M. Cheneau, B. Battelier, and J. Dalibard, *Berezinskii-Kosterlitz-Thouless crossover in a trapped atomic gas* Nature (London) **441**, 1118 (2006).
 - [6] K. Martiyanov, V. Makhalov, and A. Turlapov, *Observation of a two dimensional Fermi gas of atoms*, Phys. Rev. Lett. **105**, 030404 (2010).
 - [7] A. T. Sommer, L. W. Cheuk, M. J. H. Ku, W. S. Bakr, and M. W. Zwierlein, *Evolution of fermion pairing from three to two dimensions*, Phys. Rev. Lett. **108**, 045302 (2012).
 - [8] B. Fröhlich, M. Feld, E. Vogt, M. Koschorreck, M. Kohl, C. Berthod, and T. Giamarchi, *Two-dimensional Fermi liquid with attractive interactions*, Phys. Rev. Lett. **109**, 130403 (2012).
 - [9] V. Makhalov, K. Martiyanov, and A. Turlapov, *Ground-state pressure of quasi-2D Fermi and*

- Bose gases*, Phys. Rev. Lett. **112**, 045301 (2014).
- [10] L. Rammelmüller, W. J. Porter, and J. E. Drut, *Ground state of the two-dimensional attractive Fermi gas: Essential properties from few to many body* Phys. Rev. A **93** 033639 (2016)
- [11] S. Tung, G. Lamporesi, D. Lobser, L. Xia, and E.A. Cornell, *Observation of the Presuperfluid Regime in a Two-Dimensional Bose Gas*, Phys. Rev. Lett. **105**, 230408 (2010).
- [12] I. Boettcher, L. Bayha, D. Kedar, P.A. Murthy, M. Neidig, M. G. Ries, A. N. Wenz, G. Zürn, S. Jochim, and T. Enss, *Equation of State of Ultracold Fermions in the 2D BEC-BCS Crossover Region*, Phys. Rev. Lett. **116**, 045303 (2016).
- [13] L-C. Ha, C-L. Hung, Z. Zhang, U. Eismann, S-K. Tung and C. Chin, *Strongly Interacting Two-Dimensional Bose Gases* Phys. Rev. Lett. **110**, 145302 (2013).
- [14] J.-M. Duan, and L.-Y. Shieh, *Bound states, Cooper pairing, and Bose condensation in two dimensions*, Phys. Rev. Lett. **62**, 981 (1989).
- [15] M Randeria, J.-M. Duan, and L.-Y. Shieh, *Superconductivity in a two-dimensional Fermi gas: Evolution from Cooper pairing to Bose condensation*, Phys. Rev. B **41**, 327 (1990).
- [16] J. R. Engelbrecht and M. Randeria, *Low-density repulsive Fermi gas in two dimensions: Bound-pair excitations and Fermi-liquid behavior*, Phys. Rev. B. **45**, 12419 (1992).
- [17] J. R. Engelbrecht, M. Randeria, and L. Zhang, *Landau f function for the dilute Fermi gas in two dimensions*, Phys. Rev. B. **45**, 10135 (1992)
- [18] E. R. Anderson and J. E. Drut, *Pressure, Compressibility, and Contact of the Two-Dimensional Attractive Fermi Gas* Phys. Rev. Lett. **115**, 115301 (2015)
- [19] S. S. Botelho and C. A. R. Sá de Melo, *Vortex-antivortex lattice in ultracold fermionic gases*, Phys. Rev. Lett. **96**, 040404 (2006).
- [20] K. Miyake, *Fermi liquid theory of dilute submonolayer ^3He on thin ^4He II film dimer bound state and Cooper pairs*, Progr. Theor. Phys. **69**, 1794 (1983).
- [21] D. S. Fisher and P. C. Hohenberg, *Dilute Bose gas in two dimensions*, Phys. Rev. B. **37**, 4936 (1988).
- [22] M. Holzmann, G. Baym, J.-P. Blaizot, and F. Laloë, *Superfluid transition of homogeneous and trapped two-dimensional Bose gases*, Proc. Natl. Acad. Sci. **104**, 1476 (2007).
- [23] D. S. Petrov, M. A. Baranov, and G. V. Shlyapnikov, *Superfluid transition in quasi-two-dimensional Fermi gases*, Phys. Rev. A **67**, 031601 (2003).
- [24] V.N. Popov, *Functional Integrals in Quantum Field Theory and Statistical Physics* (Reidel,

- Dordrecht, 1983).
- [25] N. Prokof'ev, O. Ruebenacker, and B. Svistunov, *Critical Point of a Weakly Interacting Two-Dimensional Bose Gas* Phys. Rev. Lett. **87**, 270402 (2001).
 - [26] N. Prokof'ev and B. Svistunov, *Two-dimensional weakly interacting Bose gas in the fluctuation region* Phys. Rev. A **66**, 043608 (2002).
 - [27] A. Rançon and N. Dupuis, *Universal thermodynamics of a two-dimensional Bose gas*, Phys. Rev. **A85** 063607 (2012).
 - [28] E. B. Kolomeisky and J. P. Straley, *Renormalization-group analysis of the ground-state properties of dilute bose systems in d spatial dimenions*, Phys. Rev. **B46** (1992) 11749.
 - [29] P. T. How and A. LeClair, *Critical point of the two-dimensional Bose gas: an S -matrix approach*, Nucl. Phys. B824 415 (2010) [arXiv:0906.0333].
 - [30] C. N. Yang and C. P. Yang, *Thermodynamics of a One-Dimensional System of Bosons with Repulsive Delta-Function Interaction* Jour. Math. Phys. **10** 1115 (1969).
 - [31] S. Tan, *Generalized virial theorem and pressure relation for a strongly correlated Fermi gas*, Ann. Phys. **323**, (2008).
 - [32] F. Werner and Y. Castin, *General relations for quantum gases in two and three dimensions: Two-component fermions* Phys. Rev. A **86**, 013626 (2012).
 - [33] G. Bertaina and S. Giorgini, *BCS-BEC Crossover in a Two-Dimensional Fermi Gas* Phys. Rev. Lett. **106**, 110403 (2011).
 - [34] E. Marcelino, A. Nicolai, I. Roditi, A. LeClair, *Virial coefficients for Bose and Fermi trapped gases beyond the unitary limit: an S -Matrix approach*, Phys. Rev. A **90**, 053619 (2014).